AIMS Environmental Science

AIMS Environmental Science, 11(3): 342–359.
DOI: 10.3934/environsci.2024016
Received: 22 March 2024
Revised: 09 May 2024
Accepted: 17 May 2024
Published: 28 May 2024

https://www.aimspress.com/journal/environmental

Research article

Optimization of liquefaction process based on global meta-analysis and machine learning approach: Effect of process conditions and raw material selection on remaining ratio and bioavailability of heavy metals in biochar

Li Ma[1,2], Likun Zhan[1,2], Qingdan Wu[1,2], Longcheng Li[3], Xiaochen Zheng[1,2], Zhihua Xiao[1,2,*] and Jingchen Zou[1,2,*]

[1] College of Environment and Ecology, Hunan Agricultural University, Changsha, Hunan, 410128, China
[2] Key Laboratory for Rural Ecosystem Health in Dongting Lake Area of Hunan Province, Changsha 410128, China
[3] Beijing Key Laboratory of Biodiversity and Organic Farming, College of Resources and Environmental Sciences, China Agricultural University, Beijing, China

* **Correspondence:** Email: xiaozhihua@hunau.edu.cn, zou.97-0428@hunau.edu.cn; Tel: +8673184673603; Fax: +8673184673603.

Abstract: Although liquefaction technology has been extensively applied, plenty of biomass remains tainted with heavy metals (HMs). A meta-analysis of literature published from 2010 to 2023 was conducted to investigate the effects of liquefaction conditions and biomass characteristics on the remaining ratio and chemical speciation of HMs in biochar, aiming to achieve harmless treatment of biomass contaminated with HMs. The results showed that a liquefaction time of 1–3 h led to the largest HMs remaining ratio in biochar, with the mean ranging from 84.09% to 92.76%, compared with liquefaction times of less than 1 h and more than 3 h. Organic and acidic solvents liquefied biochar exhibited the greatest and lowest HMs remaining ratio. The effect of liquefaction temperature on HMs remaining ratio was not significant. The C, H, O, volatile matter, and fixed carbon contents of biomass were negatively correlated with the HMs remaining ratio, and N, S, and ash were positively correlated. In addition, liquefaction significantly transformed the HMs in biochar from bioavailable fractions (F1 and F2) to stable fractions (F3) ($P < 0.05$) when the temperature was increased to 280–330 ℃, with a

liquefaction time of 1–3 h, and organic solvent as the liquefaction solvent. N and ash in biomass were positively correlated with the residue state (F4) of HMs in biochar and negatively correlated with F1 or F2, while H, O, fixed carbon, and volatile matter were negatively correlated with F4 but positively correlated with F3. Machine learning results showed that the contribution of biomass characteristics to HMs remaining ratio was higher than that of liquefaction factor. The most prominent contribution to the chemical speciation changes of HMs was the characteristics of HMs themselves, followed by ash content in biomass, liquefaction time, and C content. The findings of this meta-analysis contribute to factor selection, modification, and application of liquefied biomass to reducing risks.

Keywords: liquefaction; heavy metal; biochar; remaining ratios; chemical speciation; liquefaction parameters; biomass characteristics; carbon neutral

1. Introduction

In recent years, the environmental issue of global warming has been intensely discussed because of the extensive use of fossil energy [1]. One of the most efficient strategies for addressing these challenges lies in diminishing its utilization by replacing with a clean, green, sustainable, and renewable energy source [2]. Progress has been made in converting renewable feedstocks into energy-intensive fuels [3], thus addressing energy security issues [4]. This, in turn, has helped to reduce the use of fossil fuels to fuel reserves, reduce fuel price volatility, and offset greenhouse gas emissions [5], promoting carbon neutrality and peak carbon performance [6].

Liquefaction to produce biochar, a renewable energy source of organic materials rich in carbon, reduces greenhouse gas emissions and advances the achievement of carbon neutrality [7]. Also, many uses of liquefied biochar will return to the environment [8]. For example, application of biochar to soil not only significantly increases soil pH, cation exchange capacity (CEC), dissolved organic carbon (DOC), and soil enzyme activities [9], but also promotes microbial abundance and plant root growth [10], being an important soil remediation material [11]. Meanwhile, the porous and functionalized surface of the resulting biochar makes it a potential candidate for construction applications [12].

Hence, the broad implementation of biochar necessitates careful consideration of various factors, in particular the possible presence of toxic HMs in biochar [13]. Environmental pollution by HMs or metalloids such as chromium (Cr), cadmium (Cd), lead (Pb), arsenic (As), copper (Cu), nickel (Ni), manganese (Mn), and zinc (Zn) is a common problem in most countries and regions [14]. Currently, the high content of HMs in these extremely accessible biomasses is a challenge [15]. For instance, biochar produced from contaminated corn stalks and rice husks contain high levels of lead [15,16]. Municipal solid waste, besides consisting of complex material as organic debris, inorganic particles, pathogens, colloidal sludge, and water [17], also contains HMs and other toxic and hazardous substances [18]. Animal waste is also rich in HMs [19]. Even so, biochar after liquefaction was reported to have a lower content of the HMs chromium, cadmium, mercury, and zinc than raw materials (RM) [20]. However, after aging of the biochar after application, its adsorption as well as the adsorption of the biochar to HMs may be reactivated again. HMs pose a potential threat to the environment and human health [21].

To produce greener and more environmentally sustainable biochar, it is crucial to improve liquefaction efficiency [22]. Understanding the RM characteristics and liquefaction process conditions is essential to control the transport and transformation of HMs in liquefied biochar [23]. In previous

studies, Li et al. [24] showed that under liquefaction conditions at 340 ℃, major HMs, e.g., 70%–98% of Zn and Cu, 71%–99% of Pb, 87%–98% of Cd, and 20%–75% of As, were concentrated in the biochar and converted to more stable fractions. Zhang et al. [25] used different solvents (H_2O and HCl) to liquefy the biomass at 210–300 ℃, and the results showed that the low temperatures and HCl favored the removal of Cd and Zn from the biochar. Wang et al. [26] showed that the reaction temperatures of 150–250 ℃ and reaction time of 0–120 min resulted in lower leachable HMs content in biochar. Song et al. [27] showed that Cu and Zn content in biochar produced from pig manure at different liquefaction temperatures (160–240 ℃) and three residence times (1, 5, and 8 h) increased with increasing temperature and time. In summary, researchers have reported various single conditions for liquefaction treatment (process temperature, pressure, and residence time). Shafizadeh et al. [28] used machine learning modeling techniques to obtain the optimal liquefaction operating conditions for maximizing the quantity and quality of biocrude. Zhou et al. [22] investigated the effect of catalysts and solvents on bioenergy production using machine learning. Luutu et al. [29] applied meta-analysis and machine learning to explore the effects and drivers of biochar on seed germination or plant growth. Zhang et al. [30] investigated the effect of hydrothermal carbonization on the transformation of phosphorus fractions of biochar species from different organic matter using meta-analysis. However, little research has been performed on the application of meta-analysis to investigate the effects of multiple liquefaction parameters on the remaining ratio and speciation of HMs in biochar, while incorporating machine learning techniques to predict the importance of different parameters.

The remaining ratio is defined as the total content of HMs in biochar related to that in the material. Considering that, here we: (1) Evaluated the effect of different liquefaction parameters on the remaining ratio of waste biochar HMs; (2) evaluated the effect of different liquefaction processes on the fraction of waste biochar HMs; (3) applied machine learning to determine the main factors and importance of the liquefaction process affecting the remaining ratio and fraction of biochar HMs.

2. Methods

2.1. Literature search and selection of relevant primary studies

Using several databases, including the China Knowledge Resource Integrated Database, Web of Science, Google Scholar, SpringerLink, and Environmental Science & Technology, Nature, Science, we searched keywords including "biochar or hydrochar" AND "liquefaction, hydrothermal carbonization, hydrothermal liquefaction, and sub/super-critical water gasification" AND "fraction and remaining ratio of heavy metals" AND "Cr, Cd, Cu, Zn, Mn, Ni, Pb, As fraction and availability".

The selected manuscripts encompass articles published between 2010 and 2023, with 56% of them published from 2019 to 2023, 11% published prior to 2016, and the remaining 33% from 2017 to 2018. The research focused on quantitatively evaluating the potential ecological hazards of HMs in biochar using the chemical fractions and remaining ratios of HMs. The study primarily focused on analyzing the term "fraction and remaining ratios of HMs in biochar". Each published manuscript's title and abstract were meticulously reviewed. Further details on the literature selection process can be found in Figure S1.

For the meta-analysis process, the literature was stringently filtered based on the following criteria: (1) The experimental designs included a minimum of three replicates to ensure analytical reliability; (2) the studies offered clear, direct comparative data between control groups devoid of liquefaction and treatment groups that underwent such processes; (3) it was imperative for biochar or hydrochar to be recognized as a critical element within the experimental framework; (4) the research was required

to engage at least one biomass under the parameters of direct liquefaction or hydrothermal treatment, and studies focusing on pyrolysis were deliberately omitted. The literature was screened according to the above requirements. Sixty-two references were incorporated into the study, including 33 municipal waste studies, 15 manure studies, and 14 plant studies. Sorted data are shown in the supporting information.

2.2. *Data extraction*

Data extraction was meticulously conducted from manuscript tables, figures, and supplementary documents. Information was directly retrieved from textual and tabular data present in the literature. For the extraction of data from graphical representations and tables, tools such as Plot Digitizer version 2.6.8 [31,32] and ABBYY FineReader 14 software were employed [33]. The information included reaction parameters (temperature, time, solvent, elemental composition, and biochemical composition of RM), material type (municipal waste, manure, or plant), biochar yield, four fraction, and remaining ratios of HMs. Each publication underwent a thorough examination by two researchers, with the requisite information subsequently logged in a Microsoft Excel spreadsheet. The geographical distribution of the experimental sites is depicted in Figure 1, along with specific site information. The main biomass of the selected literature is municipal waste, as rapid urbanization and industrialization worldwide is generating large quantities of municipal waste with high concentrations of HMs, whose treatment and utilization has become a research priority, resulting in more research literature in this area. Different regions of China face different environmental problems and resource conditions, so research is more focused.

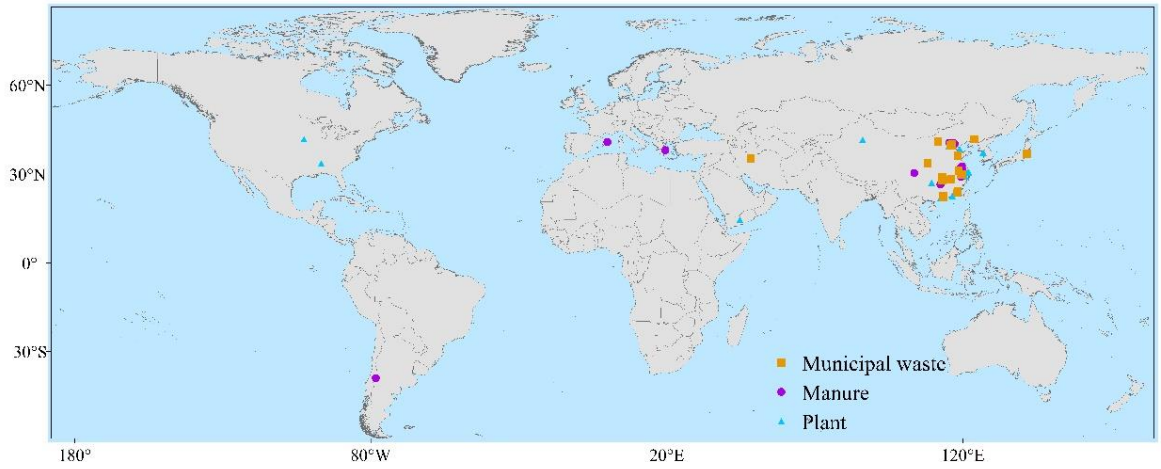

Figure 1. Geographical location of the 62 studies included in the meta-analysis.

2.3. Data statistical and meta-analysis

HMs studied in this paper included copper, zinc, manganese, nickel, cadmium, chromium, lead, and arsenic. If a certain HM is not shown in the picture in this paper, it is because the sample size of that metal was too small to draw a picture, for example, the effect of liquefaction temperature on the remaining ratio of As, the effect of liquefaction time on the remaining ratio of As and Mn, and the correlation between elemental and industrial analyses of As and Mn. According to the data distribution, the hydrothermal treatment reaction temperature, time, solvent, RM element, and industrial analysis were

divided into several categories. The following categories were used: (1) Reaction temperature (< 180 ℃, 180–229 ℃, 230–279 ℃, 280–329 ℃); (2) reaction time (duration < 1 h, 1–3 h, ≥ 3 h), (3) type of reaction solvent (water, organic solvent, acidic solvent), and (4) elemental analysis of feedstocks, biochemical composition, pH value.

The remaining ratio is defined as the total content of HMs in biochar in relation to that in the material. The remaining ratio of HMs is derived from the computation that entails the multiplication of the total HMs concentration present in the biochar by the yield of the biochar, followed by division by the total initial HMs concentration in the RM [34].

$$R\ (\%)=\frac{TB_x \times Y}{TM_x} \times 100. \quad (1)$$

X represents a specific HM, TBX denotes the total concentration of HMs within the biochar, Y signifies the yields of biochar obtained from liquefaction treatment, and TM_X refers to the total concentration of HMs present in the RM.

Linear mixed effects model analyses were used to examine the relationship between remaining ratio and liquefaction parameters, using R software (V 4.2.1). The relationships of different biomass types (municipal waste, manure, plants), HMs remaining ratio (Cd, Cr, Pb, As, Cu, Zn, Mn, and Ni), elemental composition (C, H, N, S, and O), biochemical composition (ash, volatile matter, and fixed carbon), and pH value were examined by a linear mixed-effect model, performed by the *ggplot 2* package in R. For each biomass type or HMs type, the slopes between elemental composition and biochemical composition were assembled and plotted.

Random forest model development and evaluation: The database established in Section 2.2 was used as the dataset of random forest (RF) to reveal the importance of specific variables [35]. The random forest function in the random forest package in R Studio software was used to establish the RF model [36]. The coefficient of determination (R^2) and root-mean-square error (RMSE) were employed to assess prediction accuracy and measure prediction performance [37,38]. The equations for R^2 and RMSE are given below:

$$R^2=1-\frac{\sum_{i=1}^{N}\left(m_p^i-m_t^i\right)^2}{\sum_{i=1}^{N}\left(m_t^i-m_s\right)^2}, \quad (2)$$

$$RMSE=\sqrt{\frac{\sum_{i=1}^{N}\left(m_t^i-m_p^i\right)^2}{N}}, \quad (3)$$

where m_p^i presents the forecasted output value, m_t^i denotes the actual output value obtained from the experimental research literature, m_s signifies the mean value of all output data, and N indicates the total number of data samples present in either the training or testing datasets [39]. Utilizing the RF model, potential controlling factors for the residual ratio of HMs in the liquefaction process were identified based on the relative importance of the variables.

3. Results and discussion

3.1. Effects of liquefaction parameter on HMs remaining ratio in biochar

Figures 2 and S2 summarize the statistical distribution of different liquefaction times, solvents, and temperature on HMs remaining ratio in biochar. The results show that a liquefaction time of 1–3 h is most beneficial to retain HMs in biochar. The remaining ratios mean value for Cd, Cr, Pb, Cu, Zn,

and Ni were 84.09%, 84.11%, 92.76%, 88.47%, 85.33%, and 88.22%, respectively (Figure 2). When the liquefaction time was higher than 3 h, due to biomass decomposing into smaller components while the released HMs are retained in the biochar [40], the remaining ratio was significantly ($P < 0.05$) reduced for all HMs, with the exception of Cd. The remaining ratio of Cd at >3 h was 255.70%, maybe due to the chemical reaction of the organic functional groups of Cd in the biochar forming stable or adsorbed complexes, leading to further precipitation as metal oxides or metal complexes in the biochar [41,42]. Mean values of remaining ratios for Cr, Pb, Cu, Zn, and Ni were 56.97%, 68.9%, 71.9%, and 57.31%, respectively. The longer liquefaction time may have allowed the degradation of macromolecular intermediates through compounding and secondary cracking, resulting in a decrease in the HMs remaining ratio [43]. When the liquefaction time was lower than 1 h, the HMs remaining ratio ranged from 60.76% to 85.57%. Mean values for Cd, Cr, Pb, Cu, Zn, and Ni were 60.76%, 83.22%, 75.53%, 85.57%, 64.32%, and 64.34%, respectively (Figure 2). This was probably attributed to the short reaction time where the biomass did not decompose sufficiently, resulting in a low residual rate of HMs [40].

Organic solvent led to the highest mean values, mainly in the 77.03%–93.13% range. Water solvents were often used as liquefaction solvent due to cost issues [27,44]. The mean of the remaining ratio of HMs in biochar ranged from 78.64% to 87.35% when water was used as the liquefaction solvent. In general, the liquefaction effect of biomass in organic solvents is better than that in water [45]. The acidic solvent had the lowest HMs remaining ratios, ranging from 10.59% to 80.21%, probably due to the decrease in acidity of the liquid product by the H^+ in acidic solvents, which promoted the release of HMs to the liquid phase during the liquefaction process. Hence, the order of solvents that effectively retain HMs in biochar is as follows: organic solvent > water > acidic solvent.

Figure S2 reports the HMs remaining ratio of the biochar obtained from different liquefaction temperatures. All were higher than 69.03%. The range of HMs remaining at temperatures below 180 ℃ was 70.58%–141.5% (Figure S2). The remaining ratio of Pb, Zn, and Mn decreased significantly with temperature increasing to 230–279 ℃ (69.24%, 68.27%, and 68.04%, respectively). With increasing temperature to 280–330 ℃, the remaining ratio of Pb, Zn, and Mn increased significantly ($P < 0.05$): The mean values were 81.68%, 74.40%, and 69.03%, due to HMs distributions as a result of their evaporation characteristics [46,47]. Likely, there was a facilitated hydrolysis or decomposition of organic macromolecules under higher liquefaction temperature [43]. However, liquefaction temperature had no significant ($p > 0.05$) impact on the remaining ratios of Cd, Cr, Cu, and Ni.

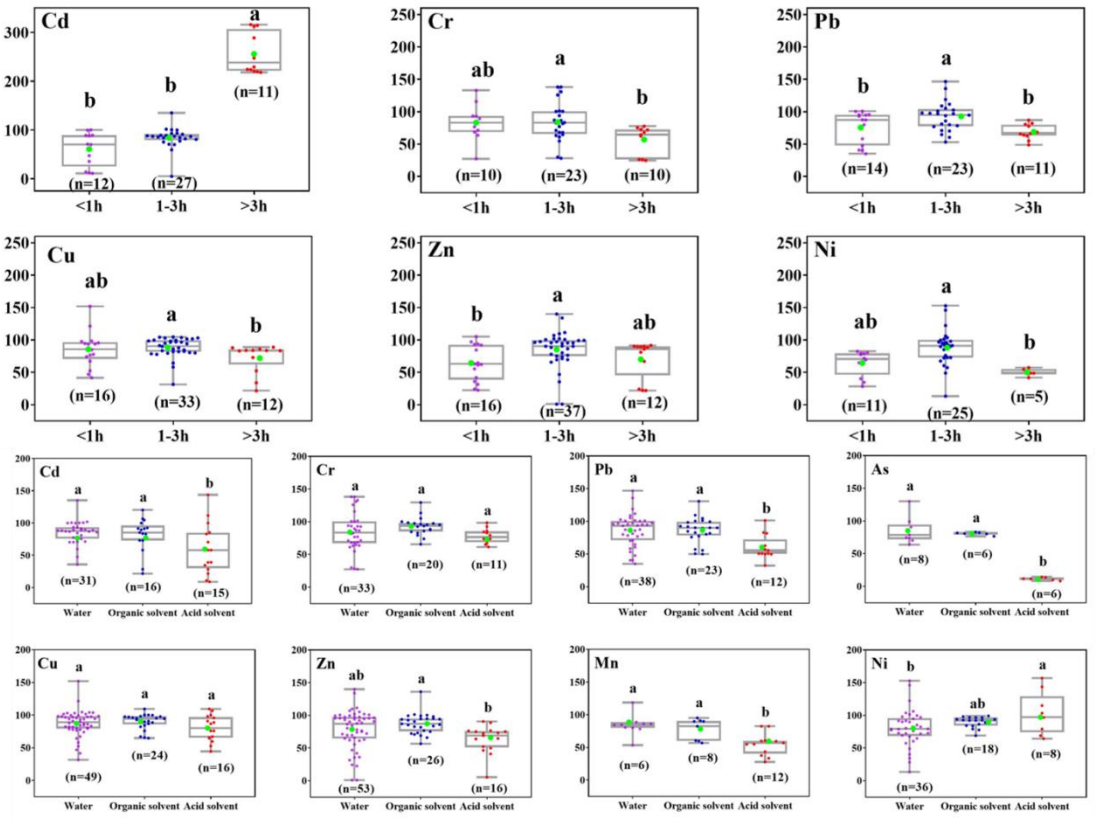

Figure 2. Effects of liquefaction time and solvents on the remaining ratio of heavy metals. The five lines from top to bottom in each boxplot represented the maximum, the third quartile (Q3), the median, the first quartile (Q1), and the minimum of statistical data, where the lowercase letters indicate significant differences ($P < 0.05$) in remaining ratio percent between different groups. The green dot indicates the mean values. The number below the box plot represents the sample size for each latitude group.

3.2. Effect of liquefaction parameter on the speciation of heavy metals in biochar

As depicted in Figure 3, the directly toxic fractions (F1 and F2) of Cd, As, Zn, Mn, and Ni exceeded 35%. In contrast, the F1 and F2 categories for Cr, Pb, and Cu are notably low in RM, with Cr and Pb concentrations being particularly minimal, at less than 10%. This indicated that over 90% of the Cr in RM was accounted for in the organic and residual phases, and Pb was principally combined with the primary minerals in RM [48]. This implies a lower environmental risk attributed to these elements within RM. Meanwhile, the Cu in RM was predominantly in the F3 fraction, attributed to its association with high-stability copper-organic complexes [49].

In relation to the HMs fractions in RM, a significant increase of the F3 or F4 fractions occurred in the biochar with temperature increase ($P < 0.05$, Figure 3). For Cd, As, Cu, Zn, and Ni in the biochar, the F3 fractions increased from 22.48%, 17.25%, 43.5%,12.35%, and 15.79% in the RM to 48.55%, 47.76%, 57.97%, 24.07%, and 27.09% in biochar, respectively, when the liquefaction temperature increased to 230–279 ℃. Some interactions (i.e., adsorption, precipitation, and complexation) might occur between the HMs and the crystal lattices of the RM with a higher liquefaction. The Pb species were mainly present in F4 (nearly 90%) as the temperature continues to rise to 280–330 ℃, but the F4 fraction percentage of Cr, Cu, and Ni in biochar greatly increased greatly 81.48%, 36.77%,

and 52.54%, respectively. This indicates that elevated liquefaction temperatures are critical controlling factors for the immobilization of HMs within biochar [50]. The aforementioned results reveal that, as the liquefaction temperature is elevated, the bioavailable fractions of HMs, namely F1 and F2, can be transposed into the stable fractions, denoted as F3 or F4.

The chemical speciation change under different liquefaction times is shown in Figure 3. The results indicate that the F3 fractions of Cu, Zn, Mn, and Ni significant increased ($P < 0.05$) from 43.70%, 13.93%, 8.85%, and 15.26% in the RM to 60.54%, 34.03%, 22.09% and 34.92% in the biochar, respectively, when the liquefaction time increases to 1–3 h. The F1 fractions of Cu, Zn, Mn, and Ni significant decreased ($P < 0.05$) from 19.45%, 28.29%, 48.66%, and 36.53% in the RM to 4.16%, 12.41%, 18.18%, and 13.21% in the biochar. Hence, a liquefaction time of 1–3 h is most beneficial for the conversion of the F1 and F2 fraction of the HMs in the RM into the stable F3 fraction. Higher or lower retention times might change the product formation pathway [38]. Different liquefaction times did not significantly ($p > 0.05$) affect the change of F4 fraction, with the exception of Cd. As can be seen from Figure 3, F4 fraction of Cd decreased significantly ($P < 0.05$) when the reaction time was extended to 1–3 h. For reaction times greater than 3 h, the F4 of Cd increased significantly ($P < 0.05$) to 65.71% compared to the RM (45.36%), accompanied by a significant decrease ($P < 0.05$) in F2 to 5.79% (22.62% for RM). This is probably because Cd is tendentiously associated with organic and sulfide substances during liquefaction process [12].

In this meta-analysis, there were relatively many studies on water as a solvent, because its use can save costs [51]. But in order to obtain higher-quality biochar, many researchers also use organic solvents [52] such as methanol, ethanol, or acetone [53]. As shown in Figure 3, using different solvents improved F3 or F4, meanwhile decreasing F1 or F2 fraction. The best results were obtained with organic solvent. Using organic solvent significantly increased ($P < 0.05$) the percentage of Cd-F3 (36.35%) and Cd-F4 (66.65%) compared with the RM Cd-F3 (24.19%) and F4 (41.34%) fraction. The F3 of Cu, Zn, and Mn increased significantly ($P < 0.05$) to 61.20%, 43.24%, and 45.15% compared to the F3 of RM: 48.77%, 21.03%, and 11.64%, Meanwhile, there was a significant decrease ($P < 0.05$) in F2 of 7.20%, 14.04%, and 14.41%, compared with 17.25%, 31.98%, and 31.97% for RM, likely due to the fact that organic solvents are polar molecules [54].

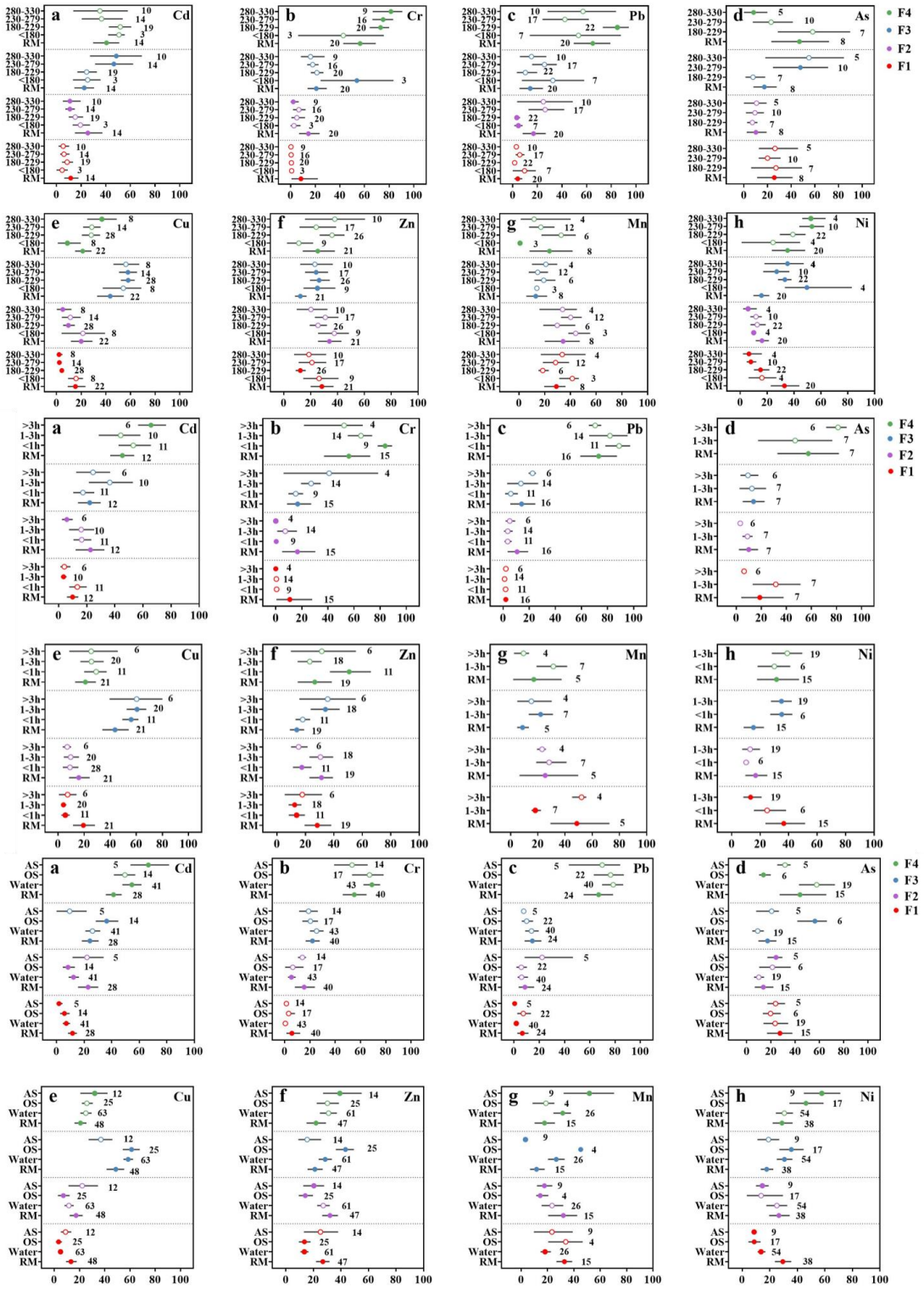

Figure 3. Effects of liquefaction parameters (liquefaction temperature, time, and solvents) on the speciation of heavy metals in biochar. Mean values and 95% CIs are shown. Filled symbols indicate a significant ($P < 0.05$) effect of reaction condition. Error bars indicate 95% CI. Each variable is presented beside each major tick label. Abbreviations: RM, raw material; OS, organic solvent; AS, acid solvent.

3.3. *Effect of raw material characteristics on the remaining ratio and speciation of heavy metals in biochar*

Correlation analyses showed that the relevant modifiers of HMs remaining ratio in biochar were C, N, S, O, ash, and fixed carbon (Figures 4 and 5). From Figure 4, it could be inferred that C, H, O, volatile matter, and fixed carbon contents are negatively correlated with the remaining ratio of HMs. The remaining ratio of some HMs was negatively correlated with the carbon element, namely Cd (slope = –1.937, R^2 = 0.374, P < 0.01, n = 21), Pb (slope = –1.104, R^2 = 0.208, P < 0.05, n = 24), Cu (slope = –0.896, R^2 = 0.155, P < 0.05, n = 36), and Ni (slope = –2.009, R^2 = 0.517, P < 0.01, n = 26), and positively correlated with N, S, and ash. The ash proportion was positively correlated with the remaining ratio of Cd (slope = 0.944, R^2 = 0.310, P < 0.01, n = 32), Cr (slope = 0.652, R^2 = 0.238, P < 0.05, n = 21), Cu (slope = 0.584, R^2 = 0.300, P < 0.01, n = 38), and Ni (slope = 0.791, R^2 = 0.445, P < 0.01, n = 29). To gain a thorough understanding of the significance of the above-mentioned factors on the remaining ratio of HMs in biochar, a prediction model was developed using machine learning methods. The relative importance of each factor and the interactions among the input variables are discussed subsequently. In addition, the variation in the F4 fraction of HMs in biochar showed a significant positive correlation with ash in biomass and a significant negative correlation (P < 0.05) with fixed carbon and volatile matter, except for Cr and Ni (Figures S3 and S4). The results indicate that biomass ash is a key control factor influencing the bioavailability of HMs in biochar.

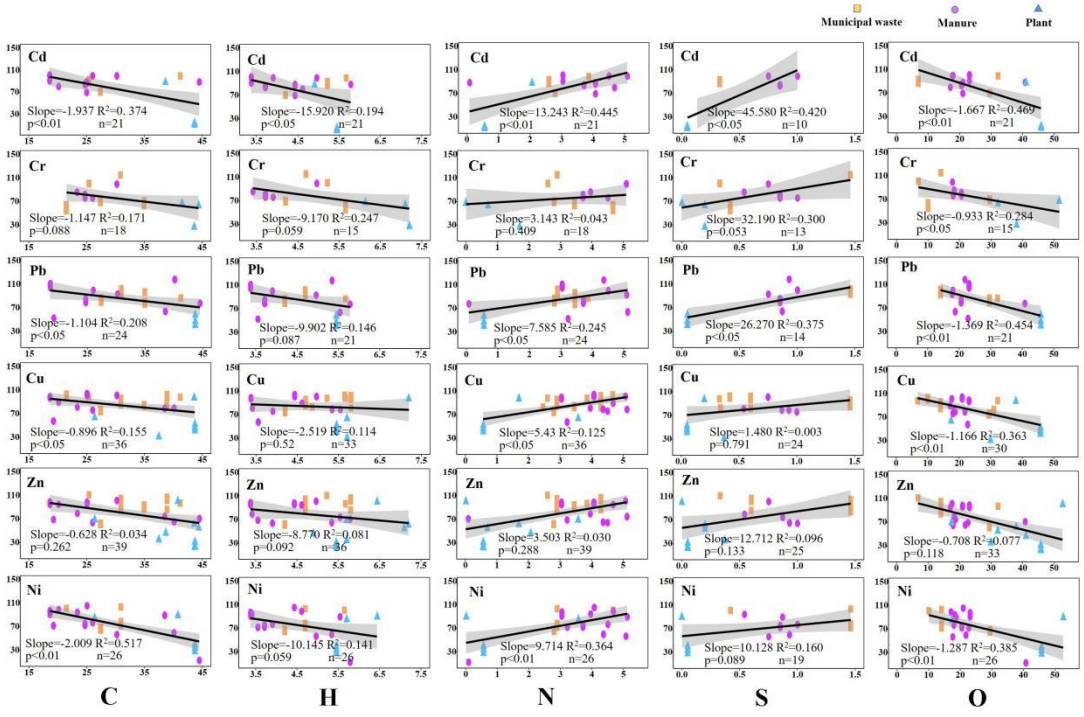

Figure 4. Correlation analysis of elemental composition (C%, H%, N%, S%, and O%) on the remaining ratio of heavy metals. Grey shading indicates the 95% confidence interval. By difference, O% = 100% – (C% + H% + N% + S% + Ash%).

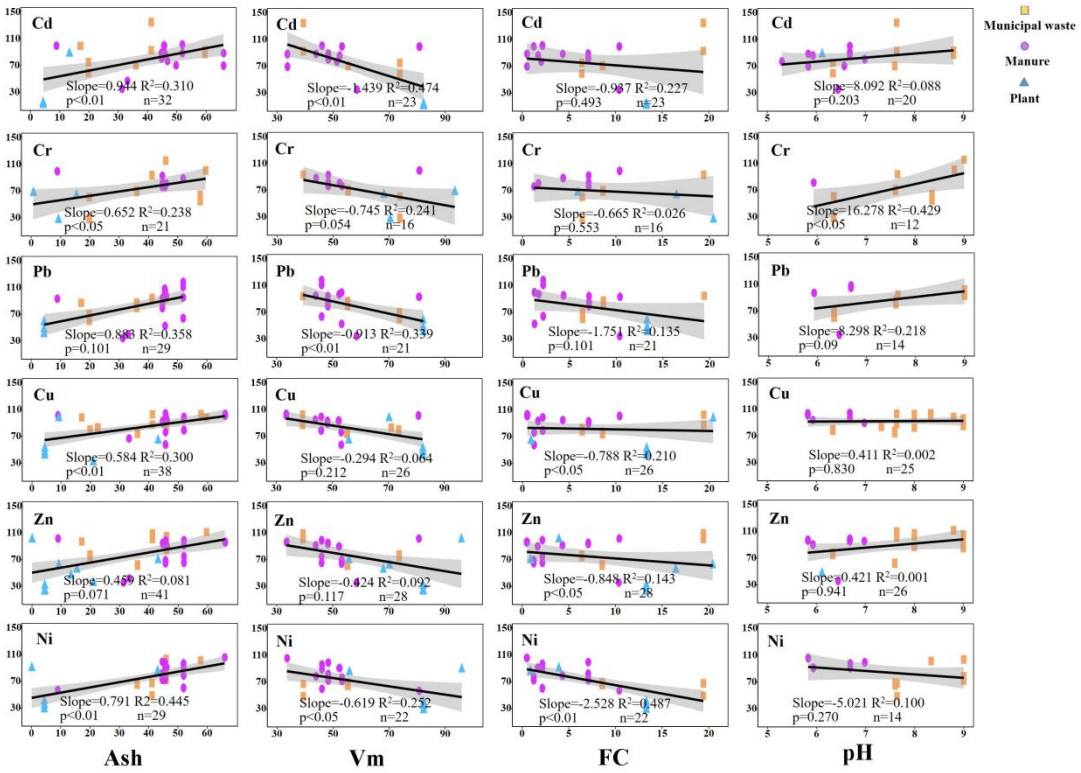

Figure 5. Correlation analysis of biochemical composition (Ash%, VM%, and FC%) and pH value on the remaining ratio of heavy metals. Grey shading indicates the 95% confidence interval. Abbreviations: Vm, volatile matter; FC, fixed carbon. Biochemical composition was based on dry basis.

3.4. Evaluation of the random forest models

The relative impact of different input parameters and RM characteristics (pH, C, H, O, N, and S contents; ash, fixed carbon, and volatile matter content) were assessed using the random forest model. Figure 6 shows that RM characteristics that have the highest importance in influencing the HMs remaining ratio. The solvent (Sl) had the smallest relative importance score. The elemental and biochemical composition accounted for as high importance as C, S, volatile matter, N, O, volatile matter, and N, being 29.81%, 28.45%, 28.45%, 22.95%, 14.72%, 22.27%, 25.16%, and 27.52% for Cd, Cr, Pb, As, Cu, Zn, and Ni, respectively, whereas the temperature and solvent had a mild effect on the remaining ratio of HMs. The importance value of temperature ranged from 3.46% to 17.11% and that of solvent from 2.88% to 11.03%.

Figure 7 demonstrates the relative importance of variables for predicting the speciation of HMs based on an enhanced random forest model developed from the dataset. The results show a relatively high accuracy of the model for the fraction of F3 (Train $R^2 = 0.819$, Train RMES = 11.478; Test $R^2 = 0.760$, Test RMES = 13.270). The chemical speciation of HMs in biochar was primarily dictated by the specific types of HMs present. To investigate this, 12 factors, namely temperature, time, solvent, ash content, fixed carbon, volatile matter, C, H, O, N, S, and pH, were selected for the construction of a random forest model to determine their importance in predicting HMs speciation. The results, depicted in Figure S5, reveal the relative importance of each variable in influencing the root mean square error (RMSE) through the use of an importance function within the random forest model. It is

evident that the characteristics of the different HMs exerted the greatest impact on the distribution of HMs into the four fractions, with an importance value exceeding 70%. Additionally, ash content, C, and time were identified as significant influencing factors for the changes in HMs fractions, with relative importance values exceeding 25%.

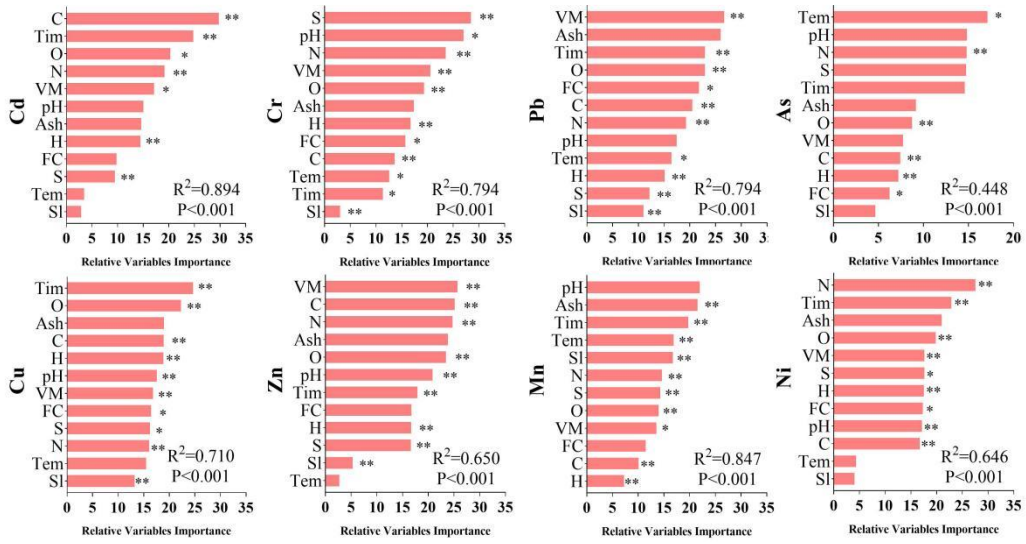

Figure 6. Feature importance from the random forest model in terms of the remaining ratio of heavy metals prediction. The machine learning algorithms were established based on data points including raw material characteristics (pH, C, H, O, N, and S contents; ash, FC, and VM content) and biochar hydrothermal process temperature, solvent, and reaction time. Significance levels of each predictor are as follows: * for $P < 0.05$ and ** for $P < 0.01$. Abbreviations: Tem, temperature; Sl, solvent; Tim, reaction time; VM, volatile matter; FC, fixed carbon.

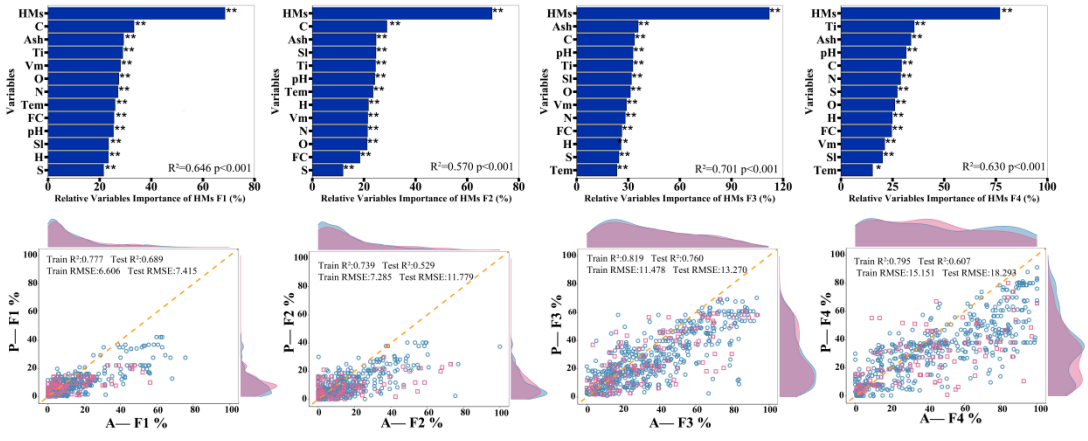

Figure 7. Relative variables importance to the prediction of HMs speciation based on improved random forest model developed from the dataset. Abbreviations: HMs, heavy metals; Tem, temperature; Sl, solvent; Tim, reaction time; VM, volatile matter; FC, fixed carbon. P-fraction indicates the predicted proportions of HMs fraction; A-fraction indicates the actual proportions of HMs fraction.

4. Conclusions

The results of this meta-analysis are summarized below:

The highest remaining ratio of HMs in biochar was observed within the 1–3 h liquefaction time, with mean values ranging from 84.09% to 92.76%. Organic solvent–liquefied biochar exhibited the greatest HMs remaining ratio, with mean values ranging from 77.03% to 93.13%; acidic solvent led to the lowest. Interestingly, the effect of liquefaction temperature on HMs remaining ratio was not significant. The C, H, O, volatile matter, and fixed carbon contents of biomass were negatively correlated with the HMs remaining ratio in biochar, and N, S, and ash were positively correlated.

The chemical speciation analysis of HMs revealed that liquefaction significantly transformed HMs from the bioavailable fractions (F1 and F2) to the stable fraction (F3) ($P < 0.05$). This transformation notably occurred when the temperature ranged from 280 to 330 °C and the liquefaction lasted for 1–3 h using organic solvent; the acid-soluble/exchangeable fractions (F1) of HMs in the biochar decreased to 2.01%–6.48%, 3.46%–18.18%, and 3.44%–13.47%. The N and ash content in biomass exhibited a positive correlation with the F4 of HMs in biochar and a negative correlation with F1 or F2.

Machine learning results indicated that both the characteristics of biomass and the characteristics of HMs themselves play a crucial role in determining the remaining ratio and chemical speciation of HMs in biochar. The impact of biomass characteristics on the remaining ratio of HMs was found to be more significant than that of the liquefaction process, with an importance value exceeding 15%. The primary factor influencing the changes in HMs speciation was the individual characteristics of different HMs, with an importance value exceeding 70%, followed by the ash content in biomass, liquefaction time, and C content, each with an importance value exceeding 25%. Therefore, a comprehensive understanding of biomass characteristics is essential before attempting to enhance the stability of HMs in biochar. By selecting appropriate liquefaction parameters, it is possible to optimize the retention of HMs in biochar while effectively mitigating the associated risks.

Based on these findings, more research is needed to better understand the transport transformation of HMs in liquefied biochar. First, the existing research consist of mainly three broad material categories—municipal waste, plants, and manure—ignoring other biomass types that may cause serious pollution; future research can redefine the types of biomass and explore them separately. In addition, synchrotron-based Fourier transform infrared and micro-X-ray fluorescence spectroscopy microscopy has been proposed to identify changes in functional groups and reveal the distribution of HMs in biosolids; their combined use can characterize the binding sites of HMs [55,56]. Therefore, future studies will aim to collect literature related to X-ray diffraction and X-ray absorption spectroscopy on biochar, to better understand the structural and speciation changes of HMs before and after treatment. Finally, current research on the transport and transformation of HMs in biochar mainly focuses on short-term ecotoxicity, being necessary to explore its long-term release properties and influencing factors by using machine learning.

Author contributions

Li Ma: Writing-original draft, Data curation, Visualization, Investigation; Likun Zhan: Investigation, Formal analysis, Software; Qingdan Wu: Investigation; Longcheng Li: Investigation; Xiaochen Zheng: Investigation; Zhihua Xiao: Writing-review & editing, Supervision; Jingchen Zou: Conceptualization, Methodology, Supervision. All authors have read and approved the final version of the manuscript for publication.

Use of AI tools declaration

The authors declare they have not used Artificial Intelligence (AI) tools in the creation of this article.

Acknowledgments

This work was financially supported by the National Key Research and Development Projects of China (2022YFD1700103), National Natural Science Foundation of China (42107435).

Conflict of interest

The authors declare no conflict of interest.

References

1. Wang X, Li C, Zhang B, et al. (2016) Migration and risk assessment of heavy metals in sewage sludge during hydrothermal treatment combined with pyrolysis. *Bioresour Technol* 221: 560–567. https://doi.org/10.1016/j.biortech.2016.09.069
2. Sharma HB, Sarmah AK, Dubey B (2020) Hydrothermal carbonization of renewable waste biomass for solid biofuel production: A discussion on process mechanism, the influence of process parameters, environmental performance and fuel properties of hydrochar. *Renew Sust Energ Rev* 123: 109761. https://doi.org/10.1016/j.rser.2020.109761
3. Castro JS, Assemany PP, Carneiro ACO, et al. (2021) Hydrothermal carbonization of microalgae biomass produced in agro-industrial effluent: Products, characterization and applications. *Sci Total Environ* 768: 144480. https://doi.org/10.1016/j.scitotenv.2020.144480
4. Wang H, Yang Z, Li X, et al. (2020) Distribution and transformation behaviors of heavy metals and phosphorus during hydrothermal carbonization of sewage sludge. *Environ Sci Pollut R* 27: 17109–17122. https://doi.org/10.1007/s11356-020-08098-4
5. Wang JX, Chen SW, Lai FY, et al. (2020) Microwave-assisted hydrothermal carbonization of pig feces for the production of hydrochar. *J Supercrit Fluid* 162: 104858. https://doi.org/10.1016/j.supflu.2020.104858
6. Tsai WT, Liu SC, Chen HR, et al. (2012) Textural and chemical properties of swine-manure-derived biochar pertinent to its potential use as a soil amendment. *Chemosphere* 89: 198–203. https://doi.org/10.1016/j.chemosphere.2012.05.085
7. Chen H, Wang X, Lu X, et al. (2018) Hydrothermal conversion of Cd-enriched rice straw and Cu-enriched Elsholtzia splendens with the aims of harmless treatment and resource reuse. *Ind Eng Chem Res* 57: 15683–15689. https://doi.org/10.1021/acs.iecr.8b04378
8. Xu X, Wu Y, Wu X, et al. (2022) Effect of physicochemical properties of biochar from different feedstock on remediation of heavy metal contaminated soil in mining area. *Surf Interfaces* 32: 102058. https://doi.org/10.1016/j.surfin.2022.102058
9. Celletti S, Bergamo A, Benedetti V, et al. (2021) Phytotoxicity of hydrochars obtained by hydrothermal carbonization of manure-based digestate. *J Environ. Manage* 280: 111635. https://doi.org/10.1016/j.jenvman.2020.111635

10. Zhang Y, Liu S, Niu L, et al. (2023) Sustained and efficient remediation of biochar immobilized with Sphingobium abikonense on phenanthrene-copper co-contaminated soil and microbial preferences of the bacteria colonized in biochar. *Biochar* 5. https://doi.org/10.1007/s42773-023-00241-x
11. Li X, Li R, Zhan M, et al. (2024) Combined magnetic biochar and ryegrass enhanced the remediation effect of soils contaminated with multiple heavy metals. *Environ Int* 185: 108498. https://doi.org/10.1016/j.envint.2024.108498
12. Li H, Yuan X, Zeng G, et al. (2010) The formation of bio-oil from sludge by deoxy-liquefaction in supercritical ethanol. *Bioresource Technol* 101: 2860–2866. https://doi:10.1016/j.biortech.2009.10.084
13. Jiang H, Yan R, Cai C, et al. (2021) Hydrothermal liquefaction of Cd-enriched Amaranthus hypochondriacus L. in ethanol-water co-solvent: Focus on low-N bio-oil and heavy metal/metal-like distribution. *Fuel* 303: 121235. https://doi.org/10.1016/j.fuel.2021.121235
14. Lee J, Park KY (2021) Conversion of heavy metal-containing biowaste from phytoremediation site to value-added solid fuel through hydrothermal carbonization. *Environ Pollut* 269: 116127. https://doi.org/10.1016/j.envpol.2020.116127
15. Fang J, Gao B, Chen J, et al. (2015) Hydrochars derived from plant biomass under various conditions: Characterization and potential applications and impacts. *Chem Eng J* 267: 253–259. https://doi.org/10.1016/j.cej.2015.01.026
16. Reza MT, Lynam JG, Uddin MH, et al. (2013) Hydrothermal carbonization: Fate of inorganics. *Biomass Bioenergy* 49: 86–94. https://doi.org/10.1016/j.biombioe.2012.12.004
17. Lang Q, Guo Y, Zheng Q, et al. (2018) Co-hydrothermal carbonization of lignocellulosic biomass and swine manure: Hydrochar properties and heavy metal transformation behavior. *Bioresource Technol* 266: 242–248. https://doi.org/10.1016/j.biortech.2018.06.084
18. Fu H, Wang B, Wang H, et al. (2022) Assessment of livestock manure-derived hydrochar as cleaner products: Insights into basic properties, nutrient composition, and heavy metal content. *J Clean Prod* 330: 129820. https://doi.org/10.1016/j.jclepro.2021.129820
19. Ren J, Wang F, Zhai Y, et al. (2017) Effect of sewage sludge hydrochar on soil properties and Cd immobilization in a contaminated soil. *Chemosphere* 189: 627–633. https://doi.org/10.1016/j.chemosphere.2017.09.102
20. Peng N, Li Y, Liu T, et al. (2017) Polycyclic aromatic hydrocarbons and toxic heavy metals in municipal solid waste and corresponding hydrochars. *Energ Fuel* 31: 1665–1671. https://doi.org/10.1021/acs.energyfuels.6b02964
21. Sun Y, Gao B, Yao Y, et al. (2014) Effects of feedstock type, production method, and pyrolysis temperature on biochar and hydrochar properties. *Chem Eng J* 240: 574–578. http://dx.doi.org/10.1016/j.cej.2013.10.081
22. Zhou X, Zhao J, Chen M, et al. (2022) Influence of catalyst and solvent on the hydrothermal liquefaction of woody biomass. *Bioresource Technol* 346: 126354. https://doi.org/10.1016/j.biortech.2021.126354
23. Hassan M, Liu Y, Naidu R, et al. (2020) Influences of feedstock sources and pyrolysis temperature on the properties of biochar and functionality as adsorbents: A meta-analysis. *Sci Total Environ* 744: 140714. https://doi.org/10.1016/j.scitotenv.2020.140714

24. Li H, Lu J, Zhang Y, et al. (2018) Hydrothermal liquefaction of typical livestock manures in China: Biocrude oil production and migration of heavy metals. *J Anal Appl Pyrol* 135: 133–140. https://doi.org/10.1016/j.jaap.2018.09.010
25. Zhang J, Wang Y, Wang X, et al. (2022) Hydrothermal conversion of Cd/Zn hyperaccumulator (Sedum alfredii) for heavy metal separation and hydrochar production. *J Hazard Mater* 423: 127122. https://doi.org/10.1016/j.jhazmat.2021.127122
26. Wang YJ, Yu Y, Huang HJ, et al. (2022) Efficient conversion of sewage sludge into hydrochar by microwave-assisted hydrothermal carbonization. *Sci Total Environ* 803: 149874. https://doi.org/10.1016/j.scitotenv.2021.149874
27. Song C, Shan S, Muller K, et al. (2018) Characterization of pig manure-derived hydrochars for their potential application as fertilizer. *Environ Sci Pollut R* 25: 25772–25779. https://doi.org/10.1007/s11356-017-0301-y
28. Shafizadeh A, Shahbeig H, Nadian MH, et al. (2022) Machine learning predicts and optimizes hydrothermal liquefaction of biomass. *Chem Eng J* 445. https://doi.org/10.1016/j.cej.2022.136579
29. Luutu H, Rose MT, McIntosh S, et al. (2021) Plant growth responses to soil-applied hydrothermally-carbonised waste amendments: A meta-analysis. *Plant Soil* 472: 1–15. https://doi.org/10.1007/s11104-021-05185-4
30. Zhang S, Wei L, Trakal L, et al. (2024) Pyrolytic and hydrothermal carbonization affect the transformation of phosphorus fractions in the biochar and hydrochar derived from organic materials: A meta-analysis study. *Sci Total Environ* 906: 167418. https://doi.org/10.1016/j.scitotenv.2023.167418
31. Lyu C, Li X, Yuan P, et al. (2021) Nitrogen retention effect of riparian zones in agricultural areas: A meta-analysis. *J Clean Prod* 315: 128143. https://doi.org/10.1016/j.jclepro.2021.128143
32. Sun G, Sun M, Du L, et al. (2021) Ecological rice-cropping systems mitigate global warming–A meta-analysis. *Sci Total Environ* 789: 147900. https://doi.org/10.1016/j.scitotenv.2021.147900
33. Liu C, Bol R, Ju X, et al. (2023) Trade-offs on carbon and nitrogen availability lead to only a minor effect of elevated CO_2 on potential denitrification in soil. *Soil Biol Biochem* 176: 108888. https://doi.org/10.1016/j.soilbio.2022.108888
34. Zeng X, Xiao Z, Zhang G, et al. (2018) Speciation and bioavailability of heavy metals in pyrolytic biochar of swine and goat manures. *J Anal Appl Pyrol* 132: 82–93. https://doi.org/10.1016/j.jaap.2018.03.012
35. Hu B, Xue J, Zhou Y, et al. (2020) Modelling bioaccumulation of heavy metals in soil-crop ecosystems and identifying its controlling factors using machine learning. *Environ Pollut* 262: 114308. https://doi.org/10.1016/j.envpol.2020.114308
36. Tang Q, Chen Y, Yang H, et al. (2021) Machine learning prediction of pyrolytic gas yield and compositions with feature reduction methods: Effects of pyrolysis conditions and biomass characteristics. *Bioresource Technol* 339: 125581. https://doi.org/10.1016/j.biortech.2021.125581
37. Li H, Wu Y, Liu S, et al. (2022) Decipher soil organic carbon dynamics and driving forces across China using machine learning. *Global Change Biol* 28: 3394–3410. https://doi.org/10.1111/gcb.16154
38. Selvam SM, Balasubramanian P (2022) Influence of biomass composition and microwave pyrolysis conditions on biochar yield and its properties: A machine learning approach. *BioEnerg Res* 16: 138–150. https://doi.org/10.1007/s12155-022-10447-9

39. Zhang W, Chen Q, Chen J, et al. (2023) Machine learning for hydrothermal treatment of biomass: A review. *Bioresource Technol* 370: 128547. https://doi.org/10.1016/j.biortech.2022.128547
40. Chen Y, Dong L, Miao J, et al. (2019) Hydrothermal liquefaction of corn straw with mixed catalysts for the production of bio-oil and aromatic compounds. *Bioresource Technol* 294: 122148. https://doi.org/10.1016/j.biortech.2019.122148
41. Chen H, Wang X, Lyu X, et al. (2019) Hydrothermal conversion of the hyperaccumulator Sedum alfredii Hance for efficiently recovering heavy metals and bio-oil. *J Environ Chem Eng* 7. https://doi.org/10.1016/j.jece.2019.103321
42. Chi T, Zuo J, Liu F (2017) Performance and mechanism for cadmium and lead adsorption from water and soil by corn straw biochar. *Front Env Sci Eng* 11. https://doi.org/10.1007/s11783-017-0921-y
43. He C, Zhang Z, Xie C, et al. (2021) Transformation behaviors and environmental risk assessment of heavy metals during resource recovery from Sedum plumbizincicola via hydrothermal liquefaction. *J Hazard Mater* 410: 124588. https://doi.org/10.1016/j.jhazmat.2020.124588
44. Lu J, Watson J, Zeng J, et al. (2018) Biocrude production and heavy metal migration during hydrothermal liquefaction of swine manure. *Process Saf Environ* 115: 108–115. https://doi.org/10.1016/j.psep.2017.11.001
45. Chen H, Zhai Y, Xu B, et al. (2014) Fate and risk assessment of heavy metals in residue from co-liquefaction of Camellia oleifera cake and sewage sludge in supercritical ethanol. *Bioresource Technol* 167: 578–581. https://doi.org/10.1016/j.biortech.2014.06.048
46. Xiao XF, Chang YC, Lai FY, et al. (2020) Effects of rice straw/wood sawdust addition on the transport/conversion behaviors of heavy metals during the liquefaction of sewage sludge. *J Environ Manage* 270: 110824. https://doi.org/10.1016/j.jenvman.2020.110824
47. Xiao Z, Yuan X, Jiang L, et al. (2015) Energy recovery and secondary pollutant emission from the combustion of co-pelletized fuel from municipal sewage sludge and wood sawdust. *Energy* 91: 441–450. https://doi.org/10.1016/j.energy.2015.08.077
48. Wang L, Chang Y, Liu Q (2019) Fate and distribution of nutrients and heavy metals during hydrothermal carbonization of sewage sludge with implication to land application. *J Clean Prod* 225: 972–983. https://doi.org/10.1016/j.jclepro.2019.03.347
49. Alipour M, Asadi H, Chen C, et al. (2021) Bioavailability and eco-toxicity of heavy metals in chars produced from municipal sewage sludge decreased during pyrolysis and hydrothermal carbonization. *Ecol Eng* 162. https://doi.org/10.1016/j.ecoleng.2021.106173
50. Shao J, Yuan X, Leng L, et al. (2015) The comparison of the migration and transformation behavior of heavy metals during pyrolysis and liquefaction of municipal sewage sludge, paper mill sludge, and slaughterhouse sludge. *Bioresource Technol* 198: 16–22. https://doi.org/10.1016/j.biortech.2015.08.147
51. Wei S, Zhu M, Fan X, et al. (2019) Influence of pyrolysis temperature and feedstock on carbon fractions of biochar produced from pyrolysis of rice straw, pine wood, pig manure and sewage sludge. *Chemosphere* 218: 624–631. https://doi.org/10.1016/j.chemosphere.2018.11.177
52. Huang HJ, Yuan XZ (2016) The migration and transformation behaviors of heavy metals during the hydrothermal treatment of sewage sludge. *Bioresource Technol* 200: 991–998. https://doi.org/10.1016/j.biortech.2015.10.099

53. Yuan X, Leng L, Huang H, et al. (2015) Speciation and environmental risk assessment of heavy metal in bio-oil from liquefaction/pyrolysis of sewage sludge. *Chemosphere* 120: 645–652. https://doi.org/10.1016/j.chemosphere.2014.10.010
54. Chen S, Chen L, Wang D, et al. (2022) Low pe+pH induces inhibition of cadmium sulfide precipitation by methanogenesis in paddy soil. *J Hazard Mater* 437: 129297. https://doi.org/10.1016/j.jhazmat.2022.129297
55. Sun FS, Yu GH, Ning JY, et al. (2020) Biological removal of cadmium from biogas residues during vermicomposting, and the effect of earthworm hydrolysates on Trichoderma guizhouense sporulation. *Bioresource Technol* 312: 123635. https://doi.org/10.1016/j.biortech.2020.123635
56. Sun FS, Yu GH, Polizzotto ML, et al. (2019) Toward understanding the binding of Zn in soils by two-dimensional correlation spectroscopy and synchrotron-radiation-based spectromicroscopies. *Geoderma* 337: 238–245. https://doi.org/10.1016/j.geoderma.2018.09.032

AIMS Press